Technical Sciences, 2020, 23(1), 69–80

UNIWERSYTET WARMIŃSKO-MAZURSKI W OLSZTYNIE

Quarterly peer-reviewed scientific journal
ISSN 1505-4675
e-ISSN 2083-4527
TECHNICAL SCIENCES
Homepage: www.uwm.edu.pl/techsci/

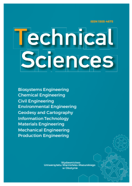

doi: 10.31648/ts.5177

THERMOVISION MEASUREMENTS OF TEMPERATURE ON THE TOOL-CHIP UPPER SIDE IN TURNING OF AISI 321 STEEL

Marian Bartoszuk

ORCID: 0000-0002-6964-6921
Faculty of Mechanical Engineering
Opole University of Technology

Received 24 February 2020, accepted 24 April 2020, available online 29 May 2020.

Keywords: cutting zone, temperature on the chip upper side, contact temperature, thermovision, infrared imaging.

Abstract

The article presents the results of thermovision tests of temperature distribution in the cutting zone. The tests were carried during orthogonal turning of AISI 321 austenitic steel without coolant. TNMA160408 inserts made of H10F carbide were selected as the cutting edges. In the study, special attention was paid to the method of determining the surface emissivity coefficient of the chip upper side. The maximum temperature values of the chip upper side determined from thermographic images were related to the average contact temperature measured by the natural thermocouple method. The results of the study indicate that the maximum temperature value of the chip upper side is proportional to the average contact temperature, and represents approximately 42-44% of its value. The results were illustrated graphically.

Correspondence: Marian Bartoszuk, Katedra Technologii Maszyn i Automatyzacji Produkcji, Wydział Mechaniczny, Politechnika Opolska, ul. Mikołajczyka 5, 45-271 Opole, phone: +48 77 449 84 61, e-mail: m.bartoszuk@po.edu.pl

Nomenclature

a_p – depth of cut [mm]
f – feed rate [mm/rev]
v_c – cutting speed [m/min]
t_k – average contact temperature [ºC]
$t_{W\max}$ – maximum temperature of the chip upper side [ºC]

Introduction

It is generally known that heat during the cutting process is generated in the primary plastic deformation zone and in the friction zone of the chip against the rake face of the cutting edge. The total amount of heat generated during the cutting process is extracted from the cutting zone by lifting together with the chip, moves to the tool cutting edge and in a negligible part flows into the workpiece (GRZESIK 2016, STEPHENSON, AGAPIOU 2016). The division of thermal streams depends both on the processing parameters and on the mutual ratio of thermo-physical properties of both tool and workpiece materials. By observing the temperature distribution in the cutting zone you get a lot of information about the cutting process itself, e.g. tool wear. Temperature distribution information can also be a valuable source of data to verify cutting simulation models. It is well known that it is difficult to measure the temperature in the cutting zone, and especially in the immediate vicinity of the contact zone. This is often done by placing a thermocouple inside the cutting edge (ANEIRO et al. 2008, YVONNET et al. 2006) but with carbide cutting edges it is not easy. Another interesting measurement technique was proposed by BASTI, OBIKAWA and SHINOZUKA (2007). To measure the average contact temperature, they used a thin thermocouple made by photolithography before applying a protective coating to the cutting edge rake face. Most often, however, the cutting temperature is measured by measuring the thermoelectric force generated at the contact between the cutting edge and the workpiece material (ABHANG, HAMEEDULLAH 2010, AKHIL et al. 2016, CEAU et al. 2010). However, this is the temperature averaged over the entire contact area, both at the rake face and clearance face. Recently, methods using IR radiation are gaining in importance. Initially, pyrometric measurements were predominant in cutting temperature measurements, but with time and the progress of electronics, thermographic and thermovision methods are becoming increasingly important (HEIGEL et al. 2017, ZHAO et al. 2018). They make it quite easy to determine the temperature distribution on the surfaces of the cutting zone, but they require a careful determination of the emissivity coefficient of the surface being tested. This necessity is due to the fact that the value of the surface emissivity coefficient has a significant impact on the measurement result (ARRAZOLA 2008, RECH 2006).

On the basis of literature data and own research results, it can be concluded that temperature measurements in the cutting zone still pose many research problems. The accuracy of the obtained measurement results depends primarily on the accuracy of the calibration of the measurement chain. In the case of thermovision measurements, the accuracy of the measurements depends on the accuracy of the determination of the emissivity coefficient of the observed surface.

This article presents problems related to thermovision measurements of temperature distribution on the surfaces of the cutting zone. Special attention has been paid to the temperature of the chip upper side as an important source of information about the cutting process itself. The sources of possible interferences and causes of measurement inaccuracies are also discussed. In the research, great emphasis was placed on developing the author's own method of determining the emissivity coefficient of the observed chip surface. Verification of the obtained results was based on the average contact temperature determined by the natural thermocouple method.

Research methodology

Workpiece and cutting tool materials

A case of dry orthogonal cutting of AISI321 austenitic steel with carbide cutting edges without protective coatings was selected for testing. The quality of the steel selected for testing was guaranteed by approval no. MEST944800/2010/. Regardless of this, the chemical composition of the steel was confirmed by laboratory tests. The results obtained are shown in Table 1. However, this steel has a high tendency to be reinforced by compression. After compression, the value of $R_{0.2}$ limit reaches 1080 to 1370 N/mm^2.

Table 1

Chemical composition of AISI 321 stainless steel

Element	Mn	Si	P	S	Cr	Ni	Mo	Cu	V	Al
% at.	1.63	0.66	0.007	0.014	17.31	9.29	0.36	0.43	0.062	0.025
Element	Ti	W	Co	Pb	Sn	As	B	N	Ca	Fe
% at.	0.309	0.029	0.116	<0.001	0.01	0.003	0.0013	<0.001	0.0017	69.70

The tests were carried out using the PTNGR 2020-16 tool holder ensuring orthogonal positioning of the TNMA 160408 cutting edge with a flat rake face (Tab. 2).

Table 2

Specification of the angles of the tool cutting edge

Cutting tool angle	Symbol	Value [°]
Normal rake	γ_n	-5
Normal clearance	α_n	5
Major tool cutting edge	κ_r	90
Inclination	λ_s	-6

As the material of the cutting edge, fine-grained H10F carbide recommended by the manufacturer, i.a., for processing steel, cast iron, stainless steel and heat-resistant alloys based on nickel, chromium and titanium with low cutting speeds and high feed rates, was adopted (*Narzędzia tokarskie* 2017).

Test stand

The tests were carried out on a stand based on a TUM-35D1 center lathe with a modernized drive system. During the tests, the values of the components of total cutting force, contact temperature and thermographic images of the cutting zone were measured and recorded. The average contact temperature was measured using the natural thermocouple method with a single cutting edge (ABHANG, HAMEEDULLAH 2010, CEAU et al. 2010). Thermographic images were collected using a JENOPTIK VarioCAM thermal imaging camera equipped with IRBIS 3 software dedicated to archiving and processing thermographic images.

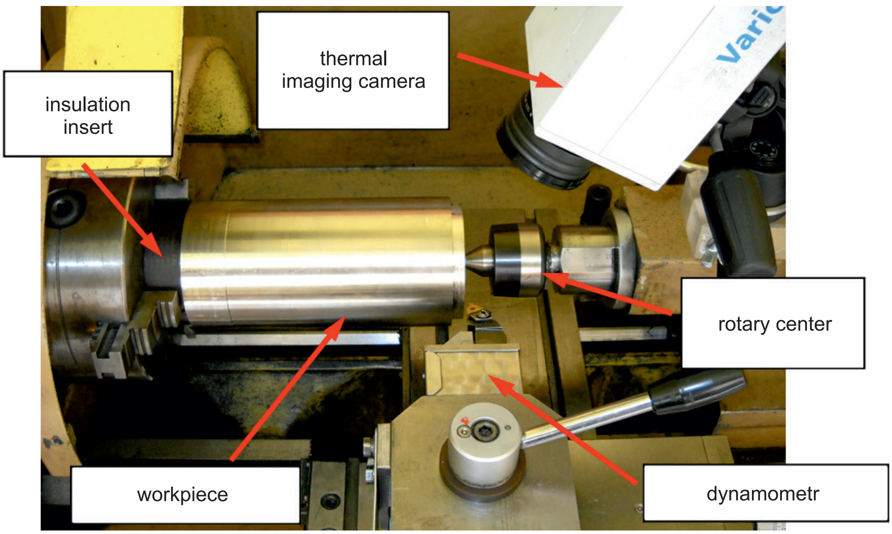

Fig. 1. View of the specimen in the processing space of the test stand

Experimental tests of the cutting process were carried out on specimens in the form of a cylinder with undercut forming a short pipe with a wall thickness of 2 mm. The location of the specimen in the test stand space is shown in Figure 1.

For the sake of recording of the tested signals a National Instruments NI 9237 measurement card and LabVIEW software were used. The selected software allowed for easy construction and adaptation of existing measurement chains to the needs of the conducted research.

Process conditions

The turning tests were carried out for orthogonal cutting, without coolant, with H10F carbide cutting edges, without protective coatings. The following processing conditions are assumed:

– cutting speed v_c = 66.67, 86.33, 100.00, 116.67, 133.33, 150.00 m/min,
– feed rate f = 0.20 mm/rev,
– cutting width a_p = 2 mm.

The samples for testing the emissivity of the chip upper side were prepared with the following cutting parameters:

– cutting speed v_c = 50.00 m/min,
– feed rate f = 0.04, 0.10, 0.16 mm/rev,
– cutting width a_p = 2 mm.

Results and discussion

Calibration of the measurement chain

During thermovision measurements of temperature distribution in the cutting zone, special attention was paid to the observation of the chip upper surface. Due to the nature of the chip forming process, its upper surface has a complex, fault-crossed texture (Fig. 2). According to the literature data (ARRAZOLA et al. 2008, M'SAOUBI et al. 2004, RECH 2006, WANG et al. 1996), the emissivity of such a surface is significantly different from that given for machined surfaces. Therefore, in order to obtain reliable temperature measurements of the chip upper side it was necessary to calibrate the measuring chain.

Typically, the calibration of thermovision measurement chains is based on a perfectly black body (M'SAOUBI et al. 2004) or specially prepared surfaces with known emissivity (WANG et al. 1996). Jaspers used a different solution in his research (JASPERS et al. 1998). The thermographic measuring chain was calibrated using a chip enclosed in a special vacuum chamber and heated by a current flow. However, these are idealized conditions, far removed from the prevailing conditions during the cutting process. Another equally impor-

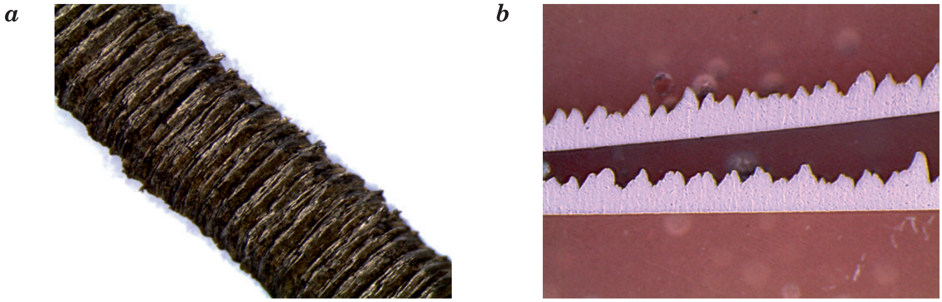

Fig. 2. The chip after orthogonal turning at a cutting speed v_c = 66.67 m/min and feed rate f = 0.1 mm/rev: a – view of the chip upper side at magnification ×10.5, b – chip longitudinal section at magnification ×24

tant aspect that can affect the accuracy of thermal imaging measurements is the oxidation of the observed surface. However, JASPERS (JASPERS et al. 1998), just like ARRAZOLA et al. (2008) have shown in their works little influence of oxidation on the change of surface emissivity coefficient.

In order to reproduce the conditions as close as possible to real conditions during calibration, the measuring chain was calibrated using chips placed on a plate made of tested steel. To reduce heat conduction losses between the substrate plate and the chip, DRAGON ceramic heat-resistant adhesive was used. As with the experimental tests during calibration, the upper side of the chips was in direct contact with the surrounding atmosphere. An overview of the calibration stand for the thermovision chain is shown in Figure 3.

The course of emission changes of the chip upper surface is shown in Table 3. The average values of chip surface emissivity produced during the experimental tests at a cutting speed v_c = 50 m/min and the values determined for the surface of a steel plate after turning were collected there. The average roughness value of the steel substrate plate was about R_a = 1.215 μm.

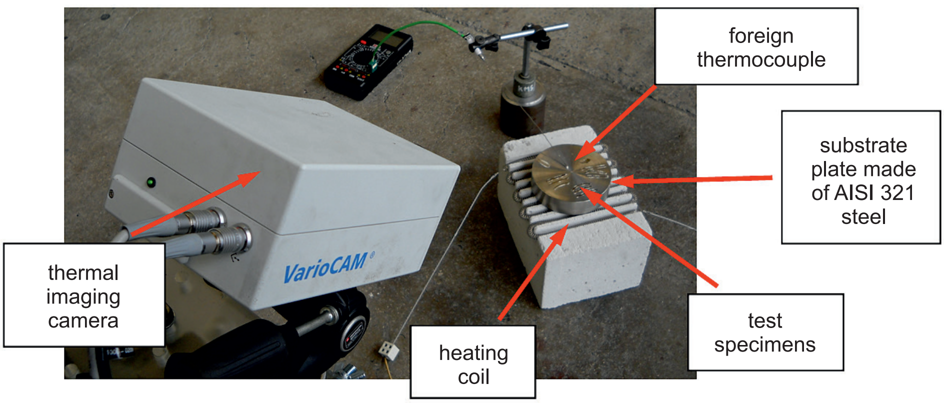

Fig. 3. A calibration stand for the thermal imaging camera

Table 3

A summary of average emissivity values of the chip surface and of AISI 321 steel after turning

Temperature [°C]	Post-turning steel	Chip surface		
		$f = 0.04$	$f = 0.10$	$f = 0.16$
50	0.24	0.50	0.53	0.58
100	0.26	0.55	0.56	0.63
150	0.25	0.54	0.54	0.59
200	0.29	0.60	0.61	0.62
250	0.28	0.59	0.57	0.61
300	0.29	0.60	0.58	0.61
350	0.29	0.63	0.58	0.61
400	0.30	0.60	0.62	0.62
450	0.30	0.58	0.57	0.58
500	0.31	0.53	0.53	0.53
550	0.37	0.49	0.50	0.49
600	0.43	0.45	0.45	0.46

The analysis of the waveform of changes in the value of the emissivity coefficient determined for the upper side of the chips indicates that regardless of the processing parameters, the observed chip surfaces have very similar emissivity values (Fig. 4). The nature of the changes, especially in the higher temperature range is almost identical for all analyzed cases. At the same time, the tests carried out indicate significant differences in the emissivity values for chips and the machined surface of the substrate plate. These differences

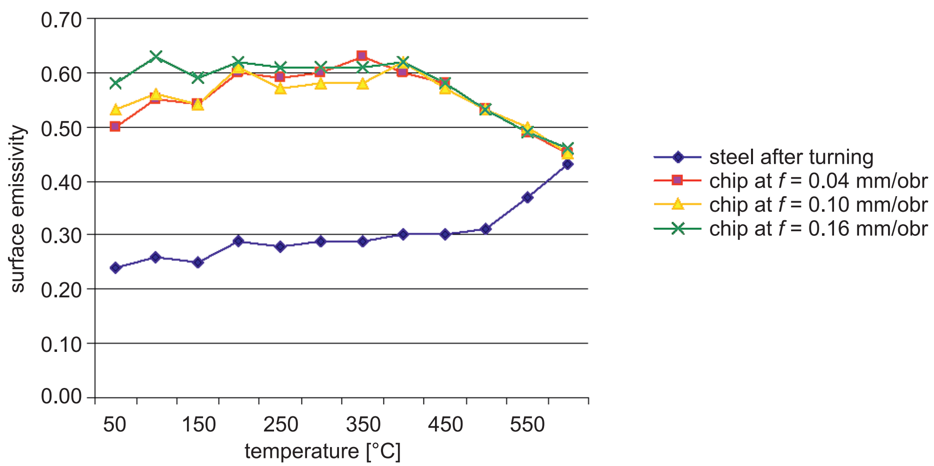

Fig. 4. The course of changes in the emissivity coefficient of the upper side of chips and AISI 321 steel after turning as a function of temperature

are particularly noticeable at temperatures below 400°C. The emissivity for the turned surface in the temperature range under consideration is about half as high as for the upper surface of the chips. Above this temperature, the difference indicated decreases noticeably.

Temperature distribution in the cutting zone

The maximum temperature generated during cutting can reach 900 or even about 1000°C. However, on the surfaces of the cutting zone we can observe much lower values. The greatest amount of heat generated in the cutting zone is carried away with the chip. Therefore, in the thermographic image of the cutting zone its surface has the brightest colors. A sample image obtained from a thermal imaging camera is shown in Figure 5. Its analysis shows that the temperature distribution along the center line of the chip is in line with the literature (JASPERS et al. 1998, RECH 2006). The waveform of the temperature changes of the upper side of the chip are shown in Figure 6. The IRBIS 3 software used in the tests allowed to automatically search for the area with the highest temperature and set the maximum temperature value. Using this function, the temperature values of the maximum chip upper side were determined for all the cases studied. An exemplary summary of the thermal imaging results and the corresponding average contact temperature values is shown in Table 4 and Figure 7.

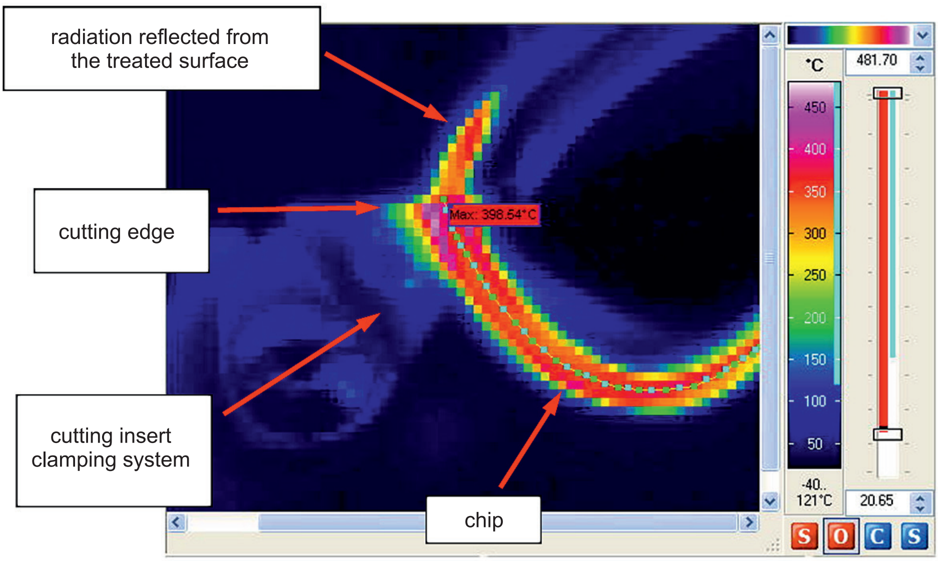

Fig. 5. A thermographic image of the cutting zone obtained for a cutting insert without coatings at a cutting speed v_c= 100 m/min and feed rate f = 0.20 mm/rev

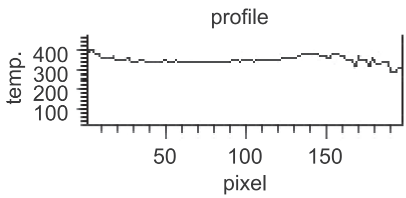

Fig. 6. The temperature distribution along the chip center line, cutting parameters: v_c = 100 m/min, f = 0.20 mm/rev

Table 4

Examples of average values of test results for a feed rate of 0.2 mm/rev and a variable cutting speed

v_c [m/min]	t_k [°C]	$t_{W\max}$ [°C]
66.67	880.0	367.3
86.33	912.4	376.5
100.00	931.0	381.8
116.67	949.4	387.3
133.33	963.1	392.1
150.00	972.0	396.3

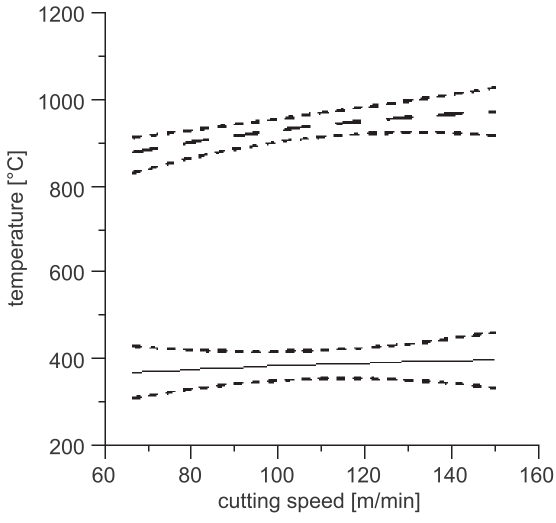

Fig. 7. Contact temperature and maximum temperature of the chip upper side; cutting parameters: v_c= 100 m/min, f = 0.20 mm/rev

When comparing the results obtained with each other, it can be seen that the temperature value of the maximum chip upper side is proportional to the average contact temperature. At cutting speed of 66.67 m/min it represents approximately 42-44% of the average contact temperature and approximately 40-42% w_k for v_c = 150 m/min. The results obtained indicate that the value of the maximum temperature of the chip upper side mainly depends on the cutting speed v_c. The feed rate does not affect the nature of changes in relation $t_{W\max}=f(t_k)$.

Interferences

Detailed analysis of the thermographic images of the cutting zone indicates that the measurement result may be affected by a number of external factors. In the previously discussed Figure 5, outside the clearly visible chip area, one can see the radiation reflected from the processed surface of the object. The cause of such an interference is considered to be the angle of the thermal imaging camera and the proximity of the heat source. The angle at which the IR camera was set during the measurements caused the collected images to show the IR radiation emitted from the chip just behind the slip zone, which was reflected on the surface of the processed test specimen. Sometimes the source of reflected radiation can be lighting or solar radiation. However, it should be noted that these interferences do not cause significant changes in the temperature distribution on the upper surface of the chip. In practice, only sporadically occurring point reflections of foreign IR radiation could be observed on the upper surface of the chip without affecting the measurement value. The negligible impact of these interferences is supposed to be due to the high roughness and irregular shape of the observed chip surface.

The literature quite often says that the reason for inaccuracies in thermal imaging measurements may be the oxidation of the observed surfaces. However, due to its relatively small importance it is usually overlooked (ARRAZOLA et al. 2008, JASPERS et al. 1998). The phenomenon of surface oxidation is closely related to the change of its emissivity coefficient. Therefore, when analyzing the nature of the changes in the surface emissivity coefficient, determined in the tests, as a function of temperature, it can be seen that the assumption made on the basis of literature data about the negligible effect of surface oxidation on the emissivity coefficient is appropriate, but only up to a temperature of about 400°C (Figure 4). When this value is exceeded, the emissivity of the chip upper surface decreases noticeably, reaching about 0.453 at 600°C. The opposite phenomenon is observed for the substrate plate. When it exceeds 450°C, its emissivity coefficient gradually increases to a value of about 0.430 at 600°C. Such changes in the emissivity coefficient values for both observed surfaces, which differ significantly in roughness, suggest that for a higher temperature range, however, the oxidation phenomenon is significant. It should be noted that the method used in the research to determine the emissivity coefficient of the upper side of the chip contained the effect of the oxidation of the observed surface, therefore additional actions to correct its value were not necessary.

The second most significant and frequent disturbing factor is the chips curling above the cutting edge. A sample image of the cutting zone with a visible chip that interferes with the measurement is shown in Figure 8. As we know, the chips may temporarily obscure the measurement site completely, making it impossible to determine the temperature in the area under study. In addition, the heat lifted along with the chip has a strong influence on the surfaces directly adjacent to it by reflecting on them and changing the temperature indication values. Due to its nature, this type of interference is difficult to control.

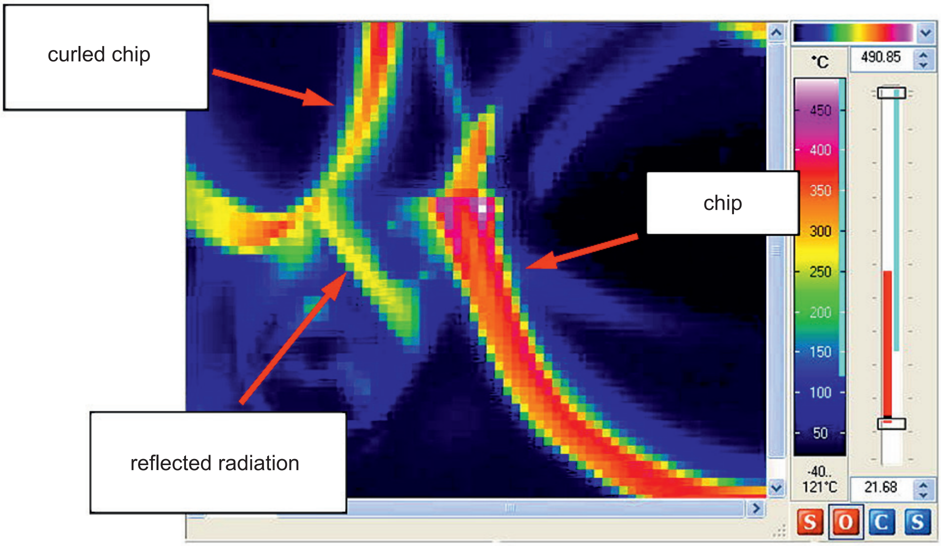

Fig. 8. The temperature distribution along the chip center line, cutting parameters: v_c = 100 m/min, f = 0.20 mm/rev

Conclusions

On the basis of the conducted research, it can be concluded that thermal imaging measurements of the temperature distribution in the cutting zone enable the determination of the maximum temperature of the chip upper side. However, the accuracy of such measurements depends on the precision of the calibration of the measuring chain. The value of the temperature determined in this way is proportional to the temperature generated with the contact area between the chips and the rake face. In the case of the examined austenitic steel, the ratio of the temperature of the chip upper side $t_{W\max}$ to the contact temperature t_k in the entire examined range of cutting speeds is almost constant and varies from

40 to 44%. It should be noted, however, that for other machined materials this ratio may take different values. The literature analysis and my own research indicate that the maximum temperature of the chip upper side can be successfully used to verify numerical calculations of the heat distribution in the cutting zone.

References

ABHANG L.B., HAMEEDULLAH M. 2010. *Chip-Tool Interface Temperature Prediction Model for Turning Process*. International Journal of Engineering Science and Technology, 2(4): 382-393.

AKHIL C.S., ANANTHAVISHNU M.H., AKHIL C.K., AFEEZ P.M., AKHILESH R., RAHUL R. 2016. *Measurement of Cutting Temperature during Machining*. IOSR Journal of Mechanical and Civil Engineering, 13(2-I): 108-122.

ANEIRO F.M., COEHO R.T., BRANDÃO L.C. 2008. *Turning Hardened Steel Using Coated Carbide at High Cutting Speeds*. Journal of the Brazilian Society of Mechanical Sciences and Engineering, XXX(2): 104-109.

ARRAZOLA P.J., ARRIOLA I., DAVIES M.A., COOKE A.L., DUTTERER B.S. 2008. *The effect of machinability on thermal fields in or-thogonal cutting of AISI 4140 steel*. CIRP Annals – Manufacturing Technology, 57: 65-68.

BASTI A., OBIKAWA T., SHINOZUKA J. 2007. *Tools with built-in thin film thermocouple sensors for monitoring cutting temperature*. International Journal of Machine Tools & Manufacture, 47: 793-798.

CEAU G., POPOVICI V., CROITORU S. 2010. *Researches About The Temperature of The Cutting Edge in Turning of Unalloyed Steel*. U.P.B. Sci. Bull., Series D, 72(3): 97-110. GRZESIK W. 2016. *Advanced Machining Processes of Metallic Materials. Theory, Modeling and Applications*. Elsevier Science.

HEIGEL J.C., WHITENTON E., LANE B., DONMEZ M.A., MADHAVAN V., MOSCOSO-KINGSLEY W. 2017. *Infrared measurement of the temperature at the tool–chip interface while machining Ti–6Al–4V*. Journal of Materials Processing Technology, 243: 123-130.

JASPERS S.P.F.C., DAUTZENBERG J.H., TAMINIAU D.A. 1998. *Temperature Measurement in Orthogonal Metal Cutting*. The International Journal of Advanced Manufacturing Technology, 14: 7-12.

M'SAOUBI R., CHANDRASEKARAN H. 2004. *Investigation of the effects of tool micro-geometry and coating on tool temperature during orthogonal turning of quenched and tempered steel*. International Journal of Machine Tools & Manufacture, 44: 213-224.

Narzędzia tokarskie. 2017. Katalog firmy Sandvik Coromant.

RECH J. 2006. *Influence of cutting tool coatings on the tribological phe-nomena at the tool-chip interface in orthogonal dry turning*. Surface & Coatings Technology, 200: 5132-5139.

STEPHENSON D.A., AGAPIOU J.S. 2016. *Metal Cutting Theory and Practice*. Third Edition, CRC Press.

WANG L., SAITO K., JAWAHIR S.I. 1996. *Infrared temperature meausrement of curled chip formation in metal machining*. Transaction of NAMRI/SME, XXIV: 87-92.

YVONNET J., UMBRELLO D., CHINESTA F., MICARI F. 2006. *A simple inverse procedure to determine heat flux on the tool in orthogonal cutting*. International Journal of Machine Tools & Manufacture, 46: 820-827.

ZHAO J., LIU Z., WANG B., HUA Y., WANG Q. 2018. *Cutting temperature measurement using an improved two-color infrared thermometer in turning Inconel 718 with whisker-reinforced ceramic tools*. Ceramics International, 44(15): 19002-19007.